Article:
Chan, EL, Washino, K, Ahmadian, H et al. (4 more authors) (2015) Dem investigation of horizontal high shear mixer flow behaviour and implications for scale-up. Powder Technology, 270 (Part B). pp. 561-568. ISSN 0032-5910

https://doi.org/10.1016/j.powtec.2014.09.017

DEM INVESTIGATION OF HORIZONTAL HIGH SHEAR MIXER FLOW BEHAVIOUR AND IMPLICATIONS FOR SCALE-UP

Ei L. Chan[1,2*], Kimiaki Washino[1,2], Hossein Ahmadian[2], Andrew Bayly[3], Zayeed Alam[2], Michael J. Hounslow[1] & Agba D. Salman[1]

1 Department of Chemical and Biological Engineering, University of Sheffield, Mappin Street, Sheffield, S1 3JD, UK

2 Procter & Gamble, Newcastle Innovation Centre, Whitley Road, Longbenton, Newcastle Upon Tyne, NE12 9BZ, UK

3 Institute of Particle Science and Engineering, University of Leeds, Leeds, LS2 9JT, U.K

*Corresponding author, Tel: +44 794 246 6264, Email: chan.e.14@pg.com

ABSTRACT

In high shear granulation, various dimensionless or dimensioned parameter groups such as constant Froude number, tip speed, relative swept volume and specific energy input are commonly used as scale-up criteria, in order to maintain the powder bed internal flow or stress field across scales. One major challenge is obtaining the internal flow and stress field through experimentation given the lack of precise measurement techniques. Hence, this work employs DEM (Discrete Element Method) simulations to study the internal flow patterns and behaviour of different scale batch, horizontal high shear mixers. The simulations provide a deeper understanding of the interaction of scale, impeller speed and fill level on the flow field, and shows that the particle velocity is correlated with the relative swept volume in these mixers. It shows that the relative particle velocity is correlated, independent of scale, to the relative swept volume per rotation and highlights its values as a parameter for understanding and comparing mixer behaviour. The work also demonstrates the importance of the particle size chosen for the simulation as well as the tool-wall gap in the mixer, and highlights its importance as we interpret DEM results.

KEYWORDS

Horizontal high shear mixer, Discrete Element Method, Particle flow, Relative swept volume, Scale-up

1. INTRODUCTION

Wet granulation or agglomeration, is a particle enlargement process used widely in detergent, pharmaceutical, food and agriculture industries, where powders are held together by inter-particle bonds with the addition of liquid binder to produce granules with enhanced properties. Amongst the wet granulation techniques, high shear mixer granulators contain mechanical blades and choppers that exerts impact and shearing forces on the granulating mixture to promote binder distribution, mixing, coalescence, granule consolidation as well as breakage. There are several high shear mixer configurations, categorised as horizontal or vertical shaft mixers and the latter can be either top- or bottom-driven [1].

In high shear granulation, maintaining the targeted product attributes upon scale-up to larger granulator usually used for production, is an important yet challenging area of study. As reviewed by several researchers [2-4], granulation scale up is typically carried out based on macroscopic approach, i.e. by controlling equipment parameters, such as operating conditions and equipment geometries. This is done by fixing one or a few dimensioned or dimensionless parameter groups as the scale up criteria. These parameters include tip speed, Froude number, relative swept volume, specific energy input, Power number, Reynolds number and spray flux [2-4]. In general, the following similarity across mixer scales should be maintained to control agglomeration conditions (besides liquid delivery conditions): geometric, kinematic (i.e. internal particle flow) and dynamic similarity (forces or energy on particles) [5]. As it is not straightforward to obtain the internal flow and stresses through experimentation, kinematic and dynamic similarity are often not discussed and established in scale-up work. Most experimental flow studies in high shear mixers are focussed on the surface flow using high speed imaging [6-10], while some studies on the internal flow were carried out mostly using the Positron Emission Particle Tracking (PEPT) technique [11-14], although this technique is costly, less accessible and limited to velocities below 2 m/s [15-16]. Advances in computer simulations, however, have enabled the internal flow, stresses, torque and mixing efficiencies to be studied via Discrete Element Method (DEM), see examples: [10-11, 13, 17-23] or Computational Fluid Dynamics (CFD), see examples: [24-25].

For scale up studies, little work has focussed on studying the internal flow [12-13, 23] and stresses/ energies [23, 26-27] in different scales vertical axis mixers. Ng et al. [12] and Hassanpour et al. [13] measured the internal flow using the PEPT method, while Nakamura et al. [23] investigated the internal flow using DEM. Both Ng et al. and Nakamura et al. found that the internal flow/kinematic similarity is maintained using constant tip speeds, i.e. a scaling exponent, n, of 1 for the impeller speed-mixer diameter scaling relationship (Equation 1), where ω and D are the impeller

speed and mixer diameter respectively. On the other hand, Tardos et al. measured the granule shear stresses indirectly by adding "test" particles known yield strength into the granulating mixture and measuring the breakage fractions [26], whilst Fu et al. inserted a probe affixed with pressure coloring films into the granule bed to measure the impact stress [27]. For constant shear stress, Tardos obtained scaling exponent, n of 0.8-0.85. Fu also obtained a value close to that for constant impact stress, i.e. n = 0.755.

$$\frac{\omega_2}{\omega_1} = \left(\frac{D_1}{D_2}\right)^n$$

Eq 1

In addition to maintaining the kinematic similarity, Nakamura et al. proposed a combined kinematic-dynamic scale up method [23]. For dynamic similarity, they proposed a constant particle collisional energy approach. They found that the averaged cumulative collisional energies, analysed with DEM, reduces with scale due to less particle circulation. With this, the process time was scaled to maintain the collisional energy. They also validated the proposed scalings experimentally.

This work is focussed on studying the internal flow of different scales batch horizontal high shear mixers using DEM, followed by kinematic similarity scaling. These are the custom-made, batch versions of continuous Lodige mixers used for manufacturing. From the literature above, most high shear mixer flow studies were for vertical shaft mixers, and this work will provide some insights on the flow in the horizontal Lodige type mixers. For simplicity, mono-sized and cohesionless particles are simulated. Figure 1 shows the mixer which contains pin tools acting as the mixing, cutting and shearing elements. Three mixer scales (Figure 2) were simulated in this work to study the impact of scale. Table 1 shows some relative dimensions of the mixers and exact geometrical details are not disclosed due to confidentially. The mixers internal diameters and volume are normalised against the smallest scale mixer (left–most in Figure 2) dimensions respectively. Note that the mixers also have a different length to diameter ratio whilst the width of the pins scales with the mixer length. The mixers contain the same number of pins. Due to the intense operation of these mixers, a sufficient gap has to be maintained between the pin tools and the mixer wall for safety purposes. Therefore, two different set of pin-wall gap ratios were studied, by keeping the gap to mixer radius, G/R, constant across scales (Table 1).

[Insert Figure 1 about here]

[Insert Figure 2 about here]

[Insert Table 1 about here]

2. SIMULATION METHOD AND SETUP

In this paper, the soft sphere DEM model for deformable particles which was originally proposed by Cundall and Strack [28], was applied to simulate the particle motion and interaction forces. The translational and rotational motions of particles are simply given by Newton's law of motion, where particles are subjected to external forces, i.e. gravitational and contact forces for dry and relatively large particles. In the soft sphere DEM model, contact forces composing of normal and tangential terms are generated when particles overlap; where the normal force include the elastic repulsion force and viscous damping while the tangential force represents the friction. For this work, an open source DEM code LIGGGHTS version 2.2.1 [29] was used and the Hertzian-Mindlin contact model with rolling friction was selected. Cohesion was not included in this work.

Table 2 shows the particle properties for the simulations. For agglomeration of detergent powder in the Lodige mixers, the powder is a typical detergent ingredients mix while the binder is a common detergent surfactant in the form of a very viscous paste, ~10Pa.s. Bulk density of a standard recipe of the powder-binder mixture is about 750kg/m^3. To maintain the same bulk density as the mixture, the particle density for the simulation was calculated from Equation 2, where the packing fraction (1-ε_b) is taken as the 0.6, i.e. the packing fraction of a bed of mono-sized, spherical particles packed by gravity.

$$\rho_p = \frac{\rho_b}{(1-\varepsilon_b)}$$

Eq 2

[Insert Table 2 about here]

Besides the impact of gap size as described previously, Table 3 lists the remaining variables studied including operating conditions and particle size. The fill levels and impeller speeds are within the typical operating range for the detergent powder agglomeration process. The fill level is

calculated on a bulk volume basis, i.e. the particle bulk volume divided by the mixer internal volume, excluding the shaft and tools volume. Again for confidentially reasons, impeller speeds are represented by the tip speeds normalised with the base tip speed of the smallest scale mixer. As a first approach to keep the flow field the same, we maintained constant fill levels and tip speeds across scales.

[Insert Table 3 about here]

A sensitivity study on the particle size was also performed, and the simulated particle sizes are given in Table 3. The minimum particle size increases with scale due the increasing number of particles that have to be simulated at the expense of computational time. The case with the largest number of particles (~1.5 million) takes about a week to run using 48 cores on a HPC cluster. The 5mm particles were used for standard comparisons across the mixer scales. Note that the starting ingredients for the detergent powders are much smaller than these sizes, i.e. 30-40micron diameter, and the larger granulated product at around 1mm. Even on this smaller equipment, it is computationally unfeasible to simulate these sizes (billions of particles) within a reasonable time scale.

3. RESULTS AND DISCUSSION

3.1 Flow pattern and solid fraction

Figure 3(a) shows the typical flow pattern at steady-state, at a cross section along the length of the V*=1 mixer. Note that the range of impeller speeds that we studied here are in the relatively high Froude number regimes, and the product generally flows in the shape of an annulus [3], producing a thin bed layer near the wall and the dominant motion being the direction of the pins rotation, i.e. tangential motion. To analyse the flow field, the time and spatially averaged normalised particle velocity (i.e. particle velocity magnitude/impeller velocity at particle position) is plotted against the normalised radial distance, i.e. r/R, (Figure 3b). The figure also plots the particle solid fraction along the normalised distance in which the particle bed layer can be assumed to be when the solid fraction is above a certain value (here, we assume ≥5%). The pin-wall gap region (shear zone) is also specified in the figure and the shaded area indicates the active or swept

region where particles could be impacted by the pins (impact zone). Within the bed layer, it can be seen that the velocity reduces towards the wall both in the active region and in the pin-wall gap or the shearing zone, whilst the solid fraction increases. In this work, no dead zones are observed for the cohesionless particles and within the range of gap size to particle diameter ratios studied (up to ~10) studied.

[Insert Figure 3 about here]

3.2 Impact of impeller speed and fill level (V*=1 mixer)

Impact of the operating conditions, i.e. impeller speed and fill level on the flow and solid fraction profile in the V*=1 mixer, are shown in Figure 4a and 4b respectively. Flow patterns are similar for the range of impeller speeds studied. Particle velocity increases and scales linearly with impeller speed within the bed layer containing bulk of the particles, i.e. dimensionless velocity profile is independent of velocity. The solid fraction profile and bed layer thickness remains the same, indicating that maximum bed compaction is achieved at these speeds with this fill level. A higher fill level increases the bed layer thickness and promotes further bed compaction. In addition, particle velocity increases slightly with fill level. This can be explained by the larger active or swept region with a thicker bed layer, resulting in a greater energy input on the particle bed and consequently, higher particle velocities. The correlation between the swept region and particle velocity will be discussed further in the next few sections.

[Insert Figure 4 about here]

3.3 Impact of mixer scale and particle size

3.3.1 Large gap size: G/R=0.074

The impact of mixer scales on the flow field and solid fraction is first investigated with a gap to mixer radius ratio, G/R, of 0.074. Figure 5 shows the normalised particle velocity and solid fraction

as a function of the normalised distance for all mixers at constant fill level of 12.7%, constant v_{tip}*=2 and d_p=5mm. The vertical lines indicate the pin edges, which correspond to G/R of 0.074. The flow pattern remains the same across mixer scales, i.e. particle velocity reduces and solid fraction increases towards the wall. However, the solid fractions and consequently bed thickness is not quite scaled even at constant fill. Despite being scaled with the mixer radius, there are still differences in the actual gap sizes and hence, shear zones in different scales. The gap to particle size ratio increases with mixer scale and results show that this promotes bed compaction, i.e. higher solid fractions in the gap and a relatively thinner bed as relative size of particle decreases. At this fill, the ratio of the bed thickness to gap size, δ/G, is 2.0-2.7 (i.e. about half of the bed thickness is in the gap). In addition, particle velocity also reduces with scale. The relationship between the velocities and solid fractions or bed thickness can again be related to the swept region explained earlier. From Figure 5, the relative swept region should reduce with mixer scale due to higher solid fractions in the gap.

[Insert Figure 5 about here]

To quantify the relative swept region [3], the relative swept volume per impeller rotation, RSVP, is calculated. To determine this for a horizontal mixer, Figure 6 shows the schematic of a cross section of the particle bed and the pins. The equation for the relative swept volume per rotation (i.e. volume swept by pins divided by the total volume per rotation) based on the particle bed or the bulk volume, $RSVP_{bulk}$, is given in Equation 3. R_t is the impeller radius, W is the single pin width, n_t is the number of pins, δ is the bed thickness, G is the gap size, R is the mixer inner radius and L is the mixer length. From DEM, the relative swept volume can also be calculated based on the actual particle volume. For mono-sized and constant density particles, this is given in Equation 4. $\sum_{R-\delta}^{R_t} N_p$ is the number of particles located in the swept region annulus and $N_{p,total}$ is the total number of particles. Since the number of the pins, n_t, and the ratio of the pin width to mixer length (W/L) are constant in the mixers studied here, the RSVP is largely affected by the gap size and bed thickness. The RSVP values displayed in Figure 7 are calculated on the particle volume basis (Equation 4) for the cases shown in the Figure 5 and it can be seen that the RSVP and normalised average velocity reduce with mixer scale.

[Insert Figure 6 about here]

$$RSVP_{bulk} = \frac{R_t W n_t (\delta - G)}{RL\delta}$$

Eq 3

$$RSVP_{par} = \frac{(\sum_{R-\delta}^{R_t} N_p) W n_t}{N_{p,Total} L}$$

Eq 4

[Insert Figure 7 about here]

Impact of particle size to the flow in the different mixers for G/R=0.074 is shown in Figure 8. The bed thickness to gap size ratio, δ/G, ranges about 2-3 and the resulting flow is sensitive to particle size in all mixers. Reducing particle size increases the gap to particle size ratio and similar to the behaviour shown in Figure 5, this leads to higher solid fractions in the gap and a thinner bed layer. Particle velocities reduce as a consequence of smaller relative swept volumes.

[Insert Figure 8 about here]

3.3.2 Small gap size: G/R=0.034

For a relatively smaller gap size and shear zone (G/R=0.034), Figures 9a and 9b show that there is less difference in the solid fractions, RSVP and consequently velocities between mixer scales at constant fill level, tip speed and particle size. At this G/R, the bed thickness to gap ratio, δ/G, now increases to >5 (Figure 10a-c). Interestingly, the solid fractions and velocities are now less sensitive to changes in particle size or gap to particle size ratio (Figure 10a-c) except for d_p=10mm in the

V*=1 mixer where the bed thickness is still noticeably larger. This could just be a discrepancy due to the particle size being unrealistically large in our smallest scale mixer to properly represent the bulk flow. Nonetheless, on the whole, we see that the gap has less impact on the overall flow field at large enough δ/G. On the hand other, when we have a case of δ/G=2-3 as shown before, flow is strongly influenced by the relatively large gap and shows sensitivity to the gap to particle size ratio, thus affecting the similarity of flow field across mixer scales (Figure 6 and 7). This also implies that selection of particle size for the DEM simulations to represent or predict the flow of smaller powder sizes is important, below a critical δ/G.

[Insert Figure 9 about here]

[Insert Figure 10 about here]

3.4 Particle velocity and relative swept volume correlation

The relative swept volume in vertical high shear granulators has been studied by several authors who also found that the specific energy input, i.e. energy input per unit mass, is correlated with the relative swept volume per second [30-32]. The relative swept volume per second is simply the relative swept volume per rotation, RSVP (in Equation 3&4), multiplied by the impeller rotational speed. The average particle velocity and relative swept volume per second calculated on a bulk volume basis (RSV_{bulk}) and particle volume basis ($RSV_{par)}$ are plotted in Figure 11a and 11b, respectively. These include all mixer scales, gap sizes, operating conditions and particle sizes. For confidentially reasons, the magnitudes are not displayed. From the figures, the particle velocity correlates linearly with the relative swept volume, in each mixer. Additionally, there is less scatter in the RSV_{par} results compared to the RSV_{bulk}, since the bulk volume calculation does not consider the bulk density variation within the bed layer. The particle velocity is linearly correlated with relative swept volumes although separate correlations are obtained for each mixer, due to lower number of impeller rotations per time with increasing scale. To normalise this effect, the normalised velocity, i.e. average particle velocity/impeller tip speed, is plotted instead with the relative swept volume per rotation, $RSVP_{par}$, and single correlation line is obtained for all mixer scales (Figure 12). This is a very useful result as relative swept volume per rotation is largely a geometric parameter. It

therefore provides a very useful way of: comparing mixer geometries, even across scale and when they are not geometrically similar, as is often the case in industry; understanding the impact of fill level; and giving insights into behaviours seen when there is build-up on the wall of mixers as is often noted.

[Insert Figure 11 about here]

[Insert Figure 12 about here]

3.5 Kinematic similarity scaling

In this work, the average particle velocity and velocity profile along the normalised radial distance is used as a measure of kinematic or internal flow similarity. Due to the influence of the pin-wall gap size on the flow field in our studied mixers, results in the previous sections have shown that constant tip speeds does not maintain kinematic similarity across mixer scales in all cases. To maintain the average particle velocity and velocity profile, the impeller speeds is scaled accordingly. Our work shows that the average velocity (normalised with the base tip speed) is proportionally related to the normalised tip speed – Figure 13 shows the results for the mixers at fill level of 12.7%, d_p=5mm and G/R=0.074. From the plot, the tip speeds to maintain the average particle velocity across mixer scales, can be obtained (e.g. for the base tip speed, v_{tip}*=1 case in the smallest scale mixer, the tip speeds in the V*=15 and V*=54 mixers have to be increased to v_{tip}*=1.4 and 1.6 respectively).

[Insert Figure 13 about here]

To determine if an impeller rotational speed-mixer diameter scaling relationship for kinematic similarity can be obtained (in the form of Equation 1), the scaled impeller speeds are plotted against the mixer diameters in log-log axes. An example is given in Figure 14 for d_p=5mm and G/R=0.074, at the different fill level and impeller speeds. Instead of the absolute values, we plot the normalised

impeller speed ($\omega^* \propto v_{tip}^*/D^*$) against D*, and good linear fittings are obtained. The scaling exponent, n is then given from the slopes of the linear fits.

[Insert Figure 14 about here]

Table 4 summarises n for different particle sizes at both G/R. For each particle size, we found that n is largely independent of the range of fill level and impeller speeds studied in this work. At G/R=0.034, n tends to 1 (i.e. constant tip speed criteria) due to little influences of the gap on the flow. The scaling is almost consistent across particle size except for d_p=10mm, which could just be a discrepancy due to overly large particles in the smallest scale mixer as explained previously. With a larger gap and shear zone (G/R=0.074), n reduces to 0.7-0.8 across particle size as the flow becomes sensitive to differences in gap to particle size ratio. This also implies that scaling the gap is important to maintain a consistent scaling exponent across particle size.

[Insert Table 4 about here]

The work presented here has focussed on studying and understanding the internal flow and maintaining kinematic similarity across our studied mixers. Further studies using DEM will be required to achieve similarity in the stress fields and energies across scales.

4. CONCLUSIONS

In this paper, DEM was employed to study the internal flow in batch, horizontal high shear mixers, using a simplified dry, mono-sized and larger particles approach. It is shown that within the range of the typical operating conditions, an annulus type flow is obtained and particle velocities reduce towards the mixer wall, both in the swept region and in the pin-wall gap. Particle velocities are largely influenced by the active or the swept region, and the normalised particle velocity is linearly correlated with the relative swept volume per rotation for the studied mixers. This result highlights the value of this, largely, geometric parameter in understanding and comparing mixer geometries and set-ups even across scales.

The study also demonstrates the importance of the pin-wall gap on the particle flow, where below a critical bed thickness to gap ratio (3 in this work), the bed flow becomes sensitive to changes in particle size or gap to particle size ratios. This also highlights that selection of particle size for the DEM simulations to represent or predict the flow of smaller powder sizes is important, below this critical bed thickness to gap ratio.

Kinematic similarity scaling is also carried out in this work and the average particle velocity and velocity profiles are used as a measure of the internal flow. At small enough relative gap size (G/R=0.034 in this work), the scaling exponent n in the impeller speed-mixer diameter scaling relationship tends to 1 which follows the constant tip criteria. n reduces with increasing gap as the flow becomes sensitive to changes in gap to particle size ratios. Finally, n is consistent across particle size with scaled gaps. Future work includes dynamic similarity (i.e. stress and/or energy) scaling using DEM and validation of the proposed scalings experimentally.

LIST OF SYMBOLS

d_p	particle diameter	[m]
D	mixer inner diameter	[m]
D*	relative mixer inner diameter (=D/D_{base})	[-]
G	pin-wall gap size	[m]
L	mixer length	[m]
n	kinematic similarity scaling exponent	[-]
n_t	number of pins	[-]
N_p	number of particles	[-]
r	radial distance	[m]
R	mixer inner radius	[m]
R_t	impeller radius	[m]

RSV_{bulk}	relative swept volume per second based on bulk volume	[s^{-1}]
RSV_{par}	relative swept volume per second based on particle volume	[s^{-1}]
$RSVP_{bulk}$	relative swept volume per impeller rotation based on bulk volume	[-]
$RSVP_{par}$	relative swept volume per impeller rotation based on particle volume	[-]
v_{tip}	impeller tip speed	[m/s]
v_{tip}*	normalised impeller tip speed (=$v_{tip}/v_{tip,base}$)	[-]
V	mixer volume	[m^3]
V*	relative mixer volume (=V/V_{base})	[-]
W	pin width	[m]
ρ_b	bulk density	[kg/m^3]
ρ_p	particle density	[kg/m^3]
δ	bed thickness	[m]
ω	impeller rotational speed	[rps]

REFERENCES

[1] D.W. Green, R. H. Perry, Perry's Chemical Engineers' Handbook, 8th ed., McGraw-Hill Publishing, New York, 2008.

[2] A. Faurea, P. York, R.C. Rowe, Process control and scale-up of pharmaceutical wet granulation processes: a review, European Journal of Pharmaceutics and Biopharmaceutics, 52 (2001) 269–277.

[3] P.R. Mort, Scale-up of binder agglomeration processes, Powder Technology, 150 (2005) 86– 103.

[4] M. Levin, Wet Granulation: End-point Determination and Scale-up, in: J. Swarbrick (Ed.) Encyclopedia of Pharmaceutical Technology, 3rd ed, Informa Healthcare, New York, 2007, pp. 4078-4098.

[5] H. Leuenberger, Scale-up of granulation processes with reference to process monitoring, Acta Pharmaceutical Technology, 29 (1983) 274–280.

[6] J.D. Litster, K.P. Hapgood, J.N. Micheals, A. Sims, M. Roberts, S.K. Kameneni, Scale-up of mixer granulators for effective liquid distribution, Powder Technology, 124 (2002) 272-280.

[7] R. Plank, B. Diehl, H. Grinstead, J. Zega, Quantifying liquid coverage and powder flux in high-shear granulators, Powder Technology, 134 (2003) 223-234.

[8] A.M. Nilpawar, G.K. Reynolds, A.D. Salman, M.J. Hounslow, Surface velocity measurement in a high shear mixer, Chemical Engineering Science, 61 (2006) 4172-4178.

[9] A. Darelius, E. Lennartsson, A. Rasmuson, I.N. Bjorn, S. Folestad, Measurement of the velocity field and frictional properties of wet masses in a high shear mixer, Chemical Engineering Science, 62 (2007) 2366-2374.

[10] E.L. Chan, G.K. Reynolds, B. Gururajan, M.J. Hounslow and A.D. Salman, Blade-granule bed stress in a cylindrical high-shear granulator: variability studies, Chemical Engineering and Technology, 35 (2012) 1435-1447.

[11] R.L. Stewart, J. Bridgwater, Y.C. Zhou, A.B. Yu, Simulated and measured flow of granules in a bladed mixer - a detailed comparison, Chemical Engineering Science, 56 (2001) 5457-5471.

[12] B.H. Ng, C.C. Kwan, Y.L. Ding, M. Ghadiri, X.F. Fan, D.J. Parker, Granular flow fields in vertical high shear mixer granulators, AICHE Journal, 54 (2008) 415–426.

[13] A. Hassanpour, C.C. Kwan, B.H. Ng, N. Rahmanian, Y.L. Ding, S.J. Antony, X.D. Jia, M. Ghadiri, Effect of granulation scale-up on the strength of granules, Powder Technology, 189 (2009) 304–312.

[14] Y. Saito, X. Fan, A. Ingram, J.P.K. Seville, A new approach to high-shear mixer granulation using positron emission particle tracking, Chemical Engineering Science, 66 (2011) 563-569.

[15] D.J. Parker, D.A. Allen, D.M. Benton, P. Fowles, P.A McNeila, M. Tan, T.D. Beynon, Developments in particle tracking using the Birmingham Positron Camera, Nuclear Instruments and Methods in Physics Research Section A: Accelerators, Spectrometers, Detectors and Associated Equipment, 392 (1997) 421-426.

[16] University of Birmingham - Nuclear Physics Research Group, Positron Emission Particle Tracking, Available from: http://www.np.ph.bham.ac.uk/pic/pept, 2012.

[17] Y.C. Zhou, A.B. Yu, R.L. Stewart, J. Bridgwater, Microdynamic analysis of the particle flow in a cylindrical bladed mixer, Chemical Engineering Science, 59 (2004) 1343-1364.

[18] Y. Sato, H. Nakamura, S. Watano, Numerical analysis of agitation torque and particle motion in a high shear mixer, Powder Technology, 186 (2008) 130–136.

[19] G.R. Chandratilleke, A.B. Yu, R.L. Stewart, J. Bridgwater, Effects of blade rake angle and gap on particle mixing in a cylindrical mixer, Powder Technology, 103 (2009) 303-311.

[20] B. Remy, J.G. Khinast, B.J. Glasser, Discrete element simulation of free flowing grains in a four-bladed mixer, AIChE Journal, 55 (2009) 2035-2048.

[21] B. Remy, B.J. Glasser, The effect of mixer properties and fill level on granular flow in a bladed mixer, AIChE Journal, 56 (2010) 336-353.

[22] A. Hassanpour, H. Tan, A. Bayly, P. Gopalkrishnan, B. Ng, M. Ghadiri, Analysis of particle motion in a paddle mixer using Discrete Element Method (DEM), Powder Technology, 206 (2011) 189–194.

[23] H. Nakamura, H. Fujii, S. Watano, Scale-up of high shear mixer-granulator based on discrete element analysis, Powder Technology, 236 (2013) 149-156.

[24] A. Darelius, A. Rasmuson, B. van Wachem, I.N. Bjorn, S. Folestad, CFD simulation of the high shear mixing process using kinetic theory of granular flow and frictional stress models, Chemical Engineering Science, 63 (2008) 2188-2197.

[25] B.H. Ng, Y.L. Ding, M. Ghadiri, Modelling of dense and complex granular flow in high shear mixer granulator - A CFD approach, Chemical Engineering Science, 64 (2009) 3622-3632.

[26] G.I. Tardos, K.P. Hapgood, O.O. Ipadeola, J.N. Michaels, Stress measurements in high-shear granulators using calibrated “test” particles: application to scale-up, Powder Technology, 140 (2004) 217-227.

[27] J. Fu, E.L. Chan, T. Song, C.M. Gilmour, M.J. Hounslow, A.D. Salman, Characterisation and measurement of impeller stress in high shear granulation, in: 9th International Symposium on Agglomeration, Sheffield, UK, 2009.

[28] P.A. Cundall, O.D.L. Strack, A discrete numerical model for granular assemblies, Geotechnique, 29 (1979) 47-65.

[29] C. Kloss, C. Goniva, LIGGGHTS – A New Open Source Dem Simulation Software, in: 5th Int. Conf. on Discrete Element Methods (DEM5), London, 2010.

[30] T. Schaefer, H.H. Bak, A. Jaegerskou, A. Kristensen, J.R. Svensson, P. Holm, H.G Kristensen, Granulation in different types of high speed mixers. Part 1: Effects of process variables and up-scaling, Pharmazeutische Industrie, 48 (1986) 1083-1089.

[31] P. Holm, Effect of impeller and chopper design on granulation in a high speed mixer, Drug Development and Industrial Pharmacy, 13 (1987) 1675-1701.

[32] G.J.B. Horsthuis, J.A.H. van Laarhoven, R.C.B.M. van Rooij, H. Vromans, Studies on upscaling parameters of the Gral high shear granulation process, International Journal of Pharmaceutics, 92 (1993) 143-150.

Figure01

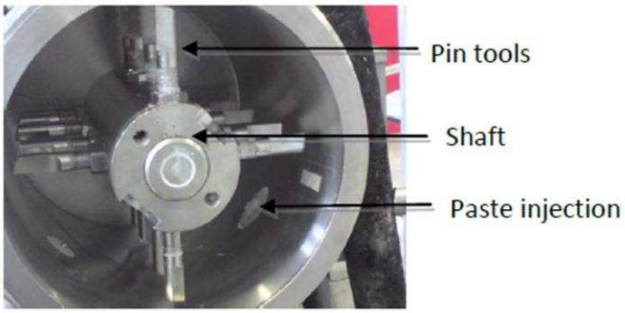

Figure 1. Custom-made, batch Lodige mixer.

Figure02

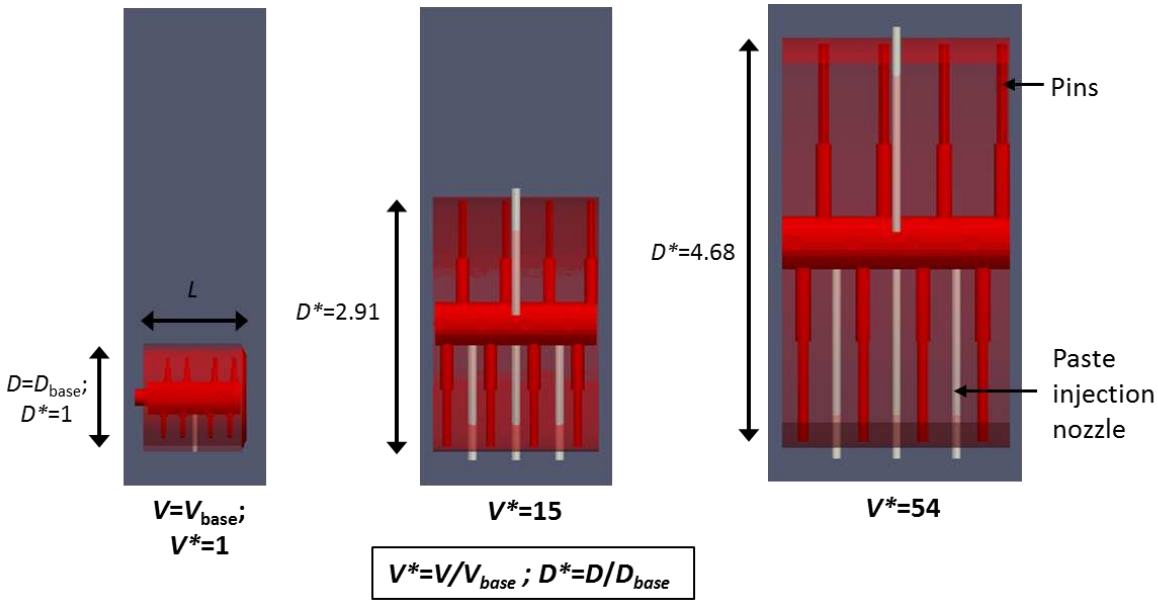

Figure 2. Mixer scales (from left): V*=1, V*=15 and V*=54.

Figure03

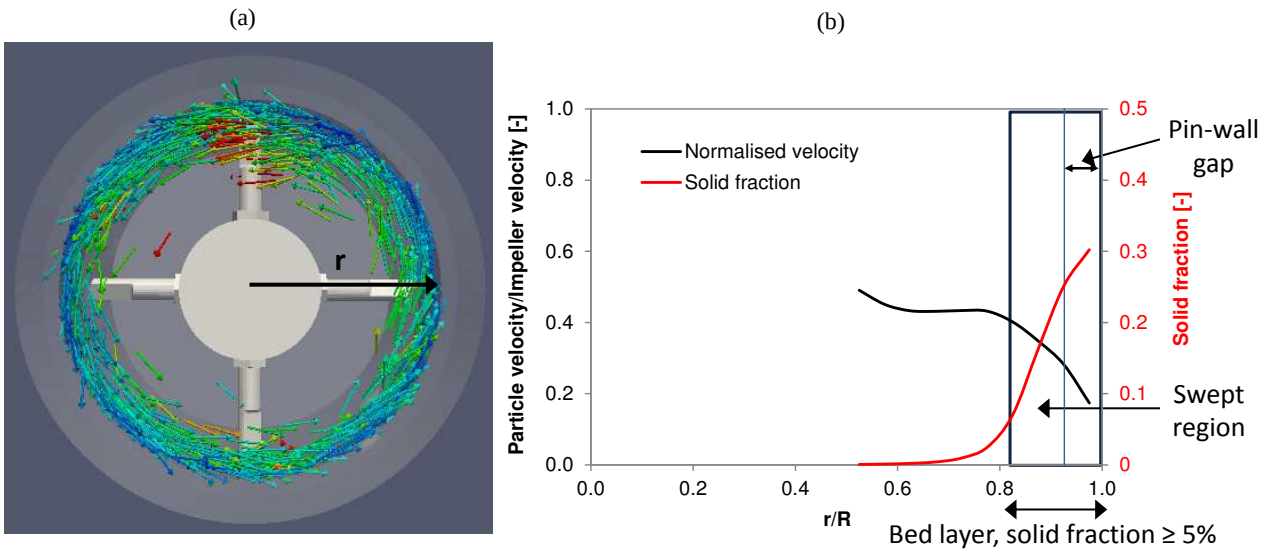

Figure 3. Flow pattern in the V*=1 mixer (a) Velocity vectors at a cross section along the mixer length and (b) Normalised particle velocity and solid fraction as a function of the normalised radial distance (FL=12.7%, v_{tip}*=2, d_p=5mm).

Figure04

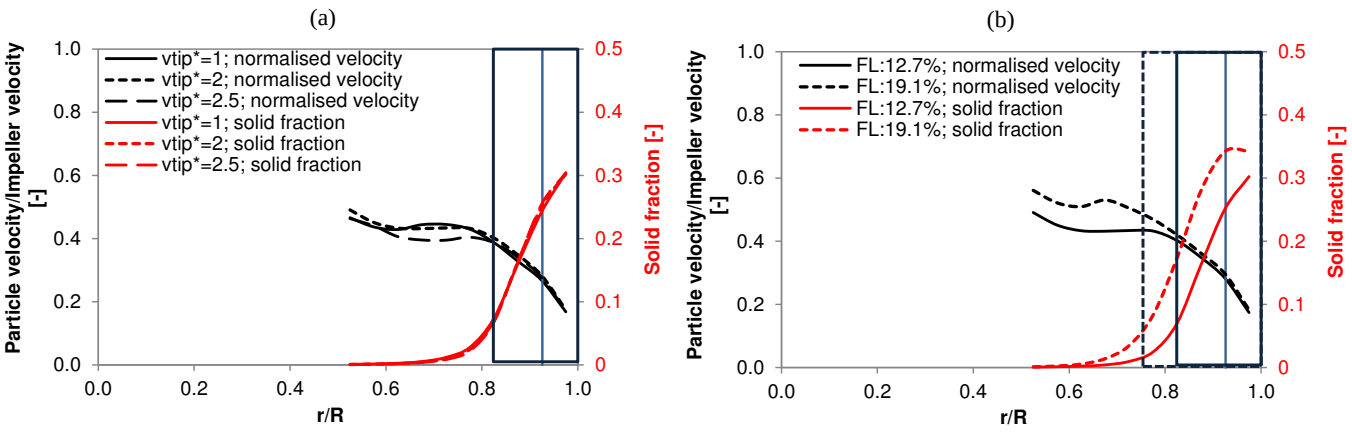

Figure 4. Normalised particle velocity and solid fraction as a function of the normalised radial distance at different (a) Impeller speed (V*=1 mixer, FL=12.7%, d_p=5mm) and (b) Fill level (V*=1 mixer, v_{tip}*=2, d_p=5mm).

Figure05

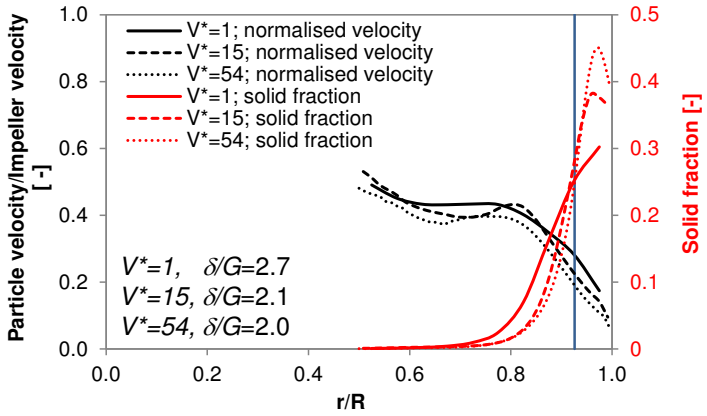

Figure 5. Comparison of mixer scales at constant fill level, tip speed and particle size: Normalised particle velocity and solid fraction as a function of the normalised radial distance (FL= 12.7%, v_{tip}*= 2, d_p=5mm, G/R=0.074).

Figure06

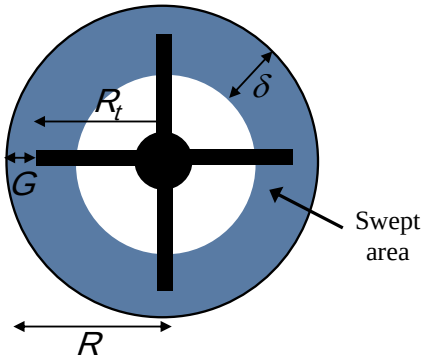

Figure 6. Cross section of the particle bed and pins in a horizontal mixer.

Figure07

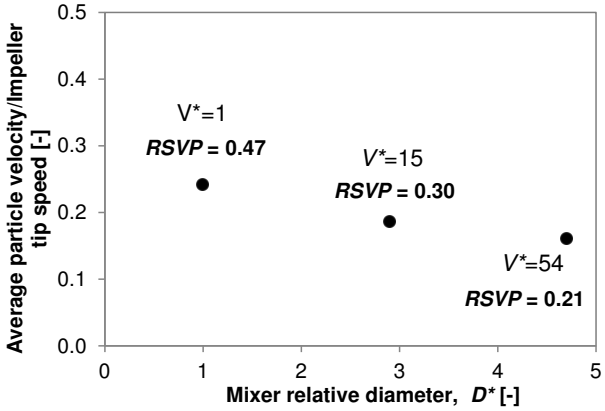

Figure 7. Comparison of mixer scales at constant fill level, tip speed and particle size: Normalised average particle velocity and calculated RSVP (FL=12.7%, v_{tip}*=2, d_p=5mm, G/R=0.074).

Figure08

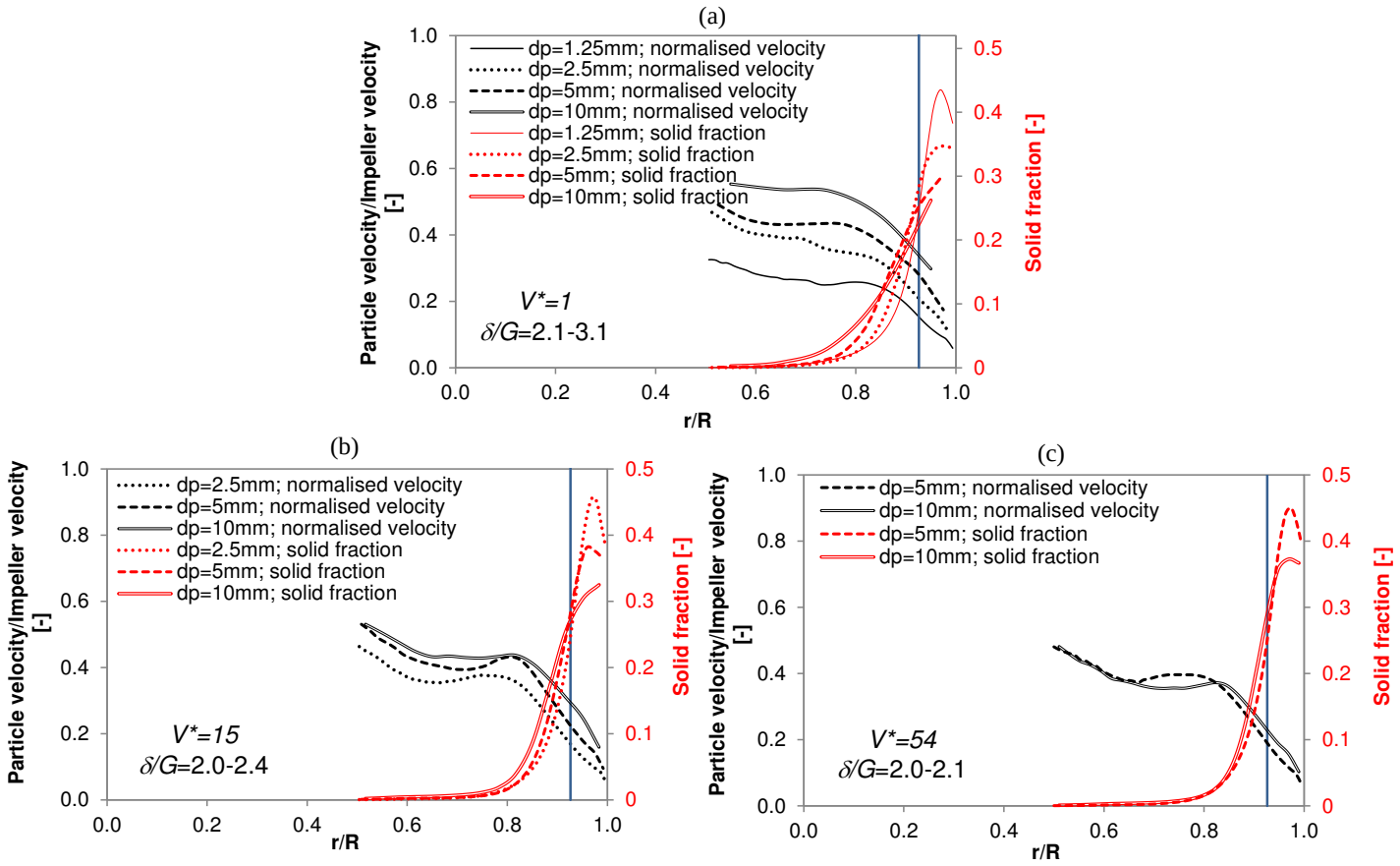

Figure 8. Normalised particle velocity and solid fraction as a function of the normalised radial distance at different particle size in the (a) V*=1 mixer (b) V*=15 mixer and (c) V*=54 mixer (FL=12.7%, v_{tip}*=2, G/R=0.074).

Figure09

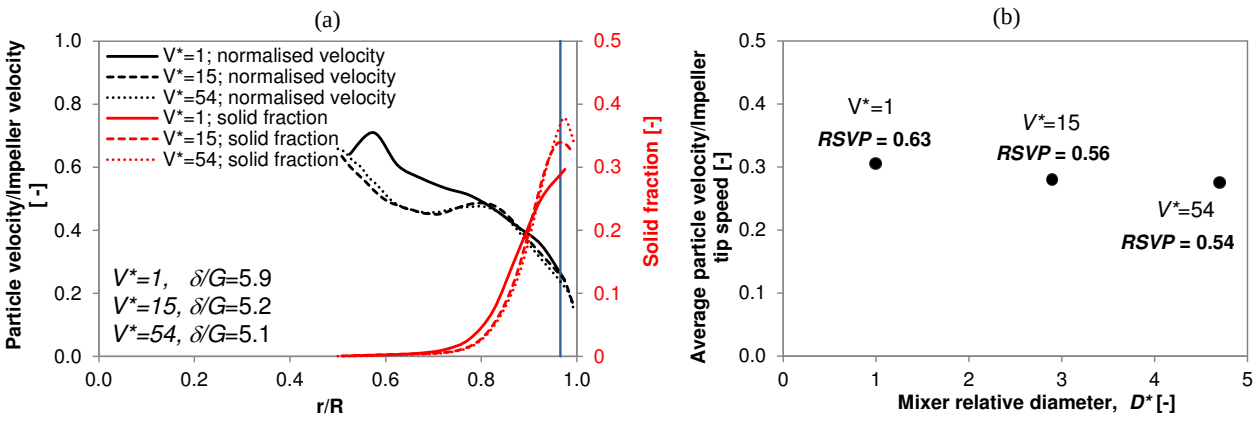

Figure 9. Comparison of mixer scales at constant fill level, tip speed and particle size: (a) Normalised particle velocity and solid fraction as a function of the normalised radial distance and (b) Normalised average particle velocity and calculated RSVP (FL=12.7%, v_{tip}*=2, d_p=5mm, G/R=0.034).

Figure10

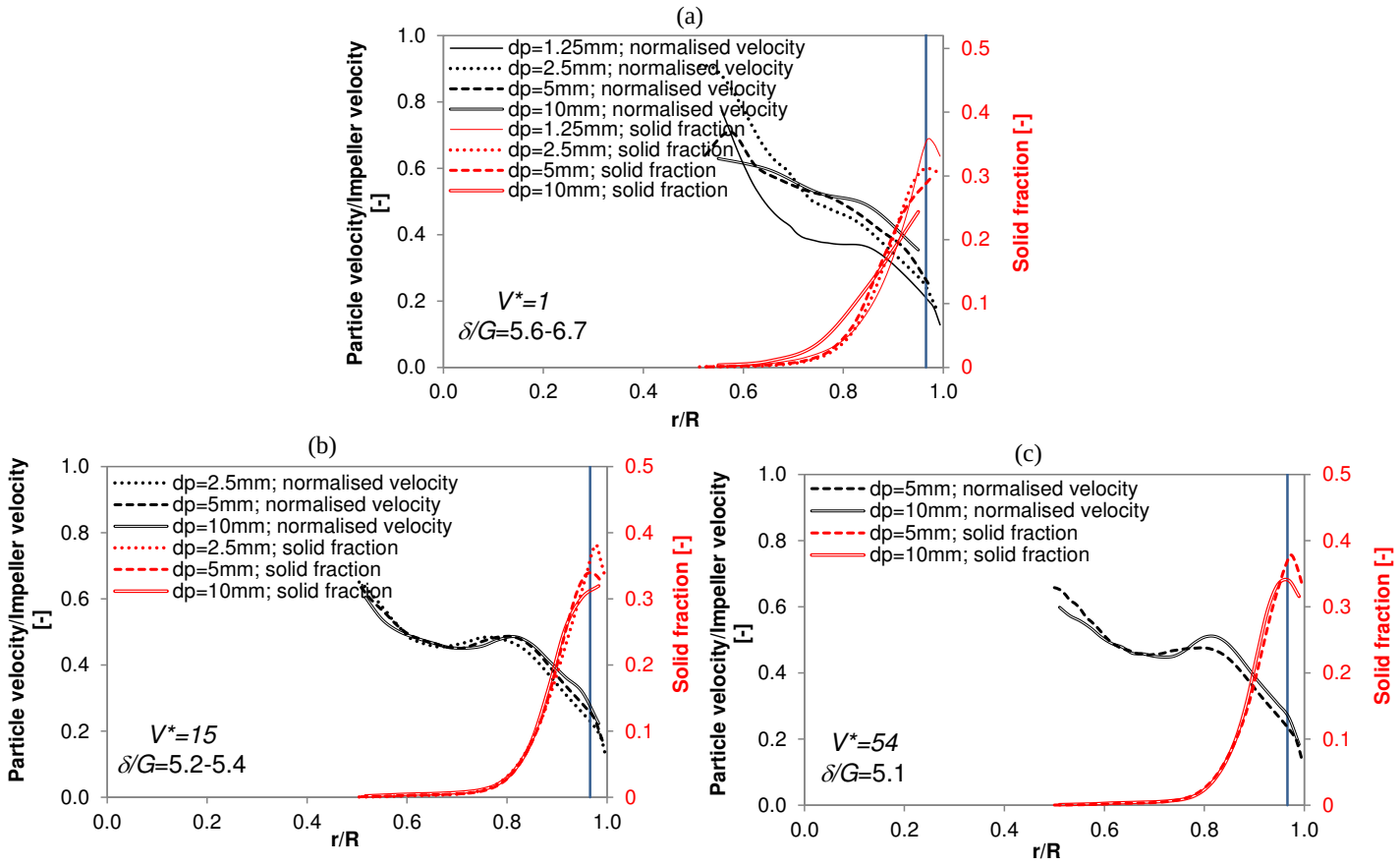

Figure 10. Normalised particle velocity and solid fraction as a function of the normalised radial distance at different particle size in the (a) V*=1 mixer (b) V*=15 mixer and (c) V*=54 mixer (FL=12.7%, v_{tip}*=2, G/R=0.034).

Figure11

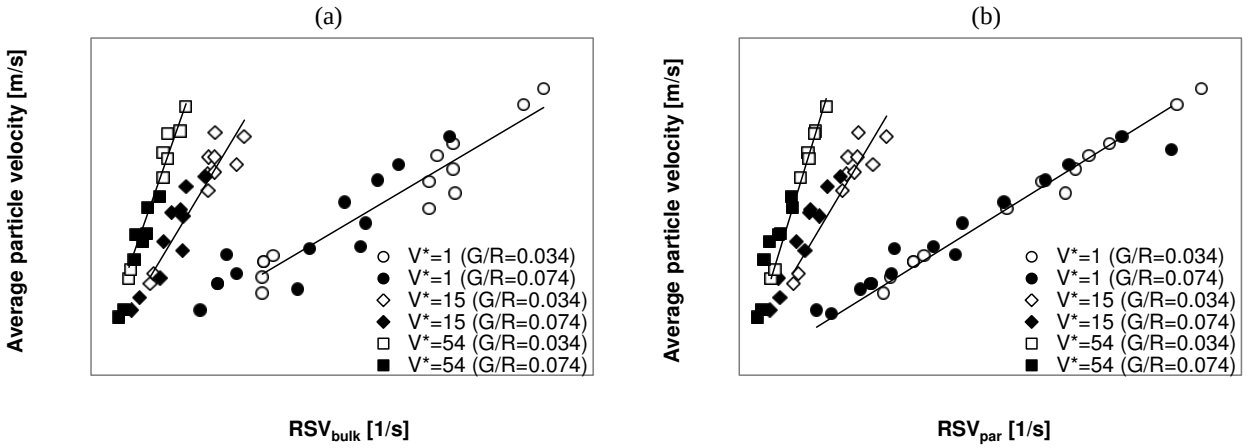

Figure 11. Plot of average particle velocity with (a) RSV_{bulk} and (b) RSV_{par}, for all mixers, gap size, operating conditions and particle size.

Figure12

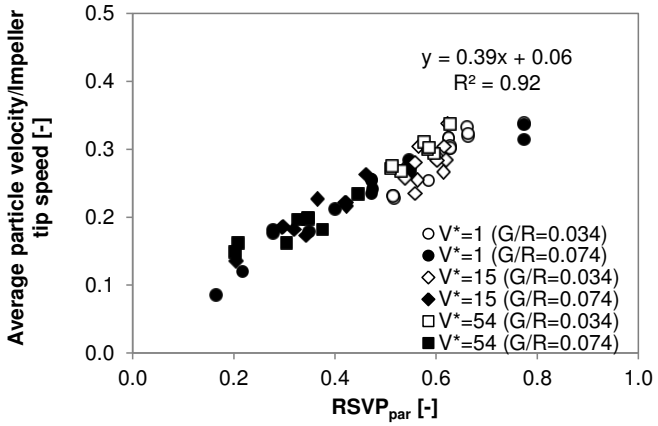

Figure 12. Plot of normalised average particle velocity vs $RSVP_{par}$ for all mixers, gap size, operating conditions and particle size.

Figure13

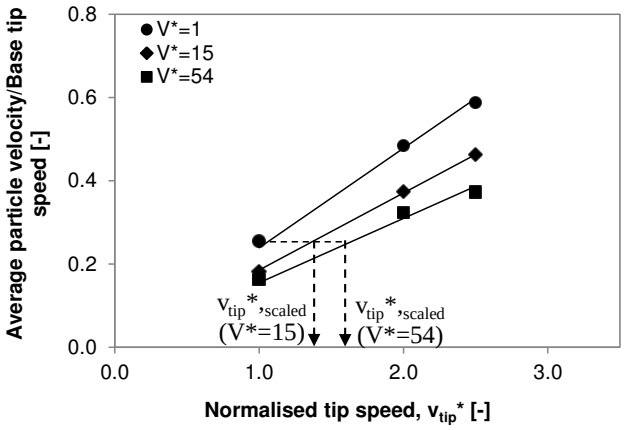

Figure 13. Kinematic similarity scaling method: Average particle velocity/base tip speed vs normalised tip speed for different mixers (FL=12.7%, d_p=5mm, G/R=0.074).

Figure14

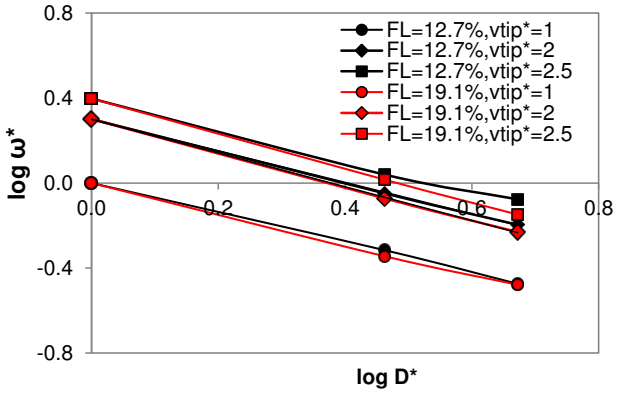

Figure 14. Example of log ω*-log D* plot (d_p=5mm, G/R=0.074) *Normalised tip speeds given in the legend are for the V*=1 mixer.

Table01

Table 1. Mixer and pin geometry.

Mixer relative volume, V* [-] [a]	Mixer relative internal diameter, D* [-] [b]	No. of pins [-]	Gap/mixer radius, G/R [-]
1	1	16	0.034, 0.074
15	2.9	16	0.034, 0.074
54	4.7	16	0.034, 0.074

[a] $V^*=V/V_{base}$; [b] $D^*=D/D_{base}$

Table02

Table 2. DEM input parameters.

Particle density (kg/m^3)	1250
Particle Young's modulus (MPa)	10
Particle Poisson's ratio (-)	0.25
Wall Young's modulus (MPa)	10
Wall Poisson's ratio (-)	0.3
Particle-particle restitution coefficient (-)	0.4
Particle-wall restitution coefficient (-)	0.4
Particle-particle sliding friction coefficient (-)	0.5
Particle-wall sliding friction coefficient (-)	0.5
Particle-particle rolling friction coefficient (-)	0.1
Particle-wall rolling friction coefficient (-)	0.1
Simulation time step (s)	$1x10^{-5}$

Table03

Table 3. Studied variables: Operating conditions, gap size and particle diameter.

Mixer relative volume, V* [-]	Fill level, FL (excl. shaft & tools) [%]	Normalised impeller tip speed, v_{tip}^{*} [-] [a]	Gap/mixer radius, G/R [-]	Particle diameter, d_p [mm]
1	12.7, 19.1	1, 2, 2.5	0.034, 0.074	1.25, 2.5, 5, 10
15	12.7, 19.1	1, 2, 2.5	0.034, 0.074	2.5, 5, 10
54	12.7, 19.1	1, 2, 2.5	0.034, 0.074	5, 10

[a] $v_{tip}^{*} = v_{tip}/v_{tip,base}$

Table04

Table 4. Summary of the scaling exponent, n.

d_p [mm]	n	
	G/R = 0.074	G/R = 0.034
10	0.7-0.8	0.8-0.9
5	0.7-0.8	0.9-1
2.5	0.75-0.8 [a]	0.9-1 [a]

[a] Data from the V*=1 and V*=15 mixers only.